Advances and Trends in STRUCTURAL and SOLID MECHANICS

Edited by

A. K. NOOR and J. M. HOUSNER
NASA Langley Research Center, U.S.A.

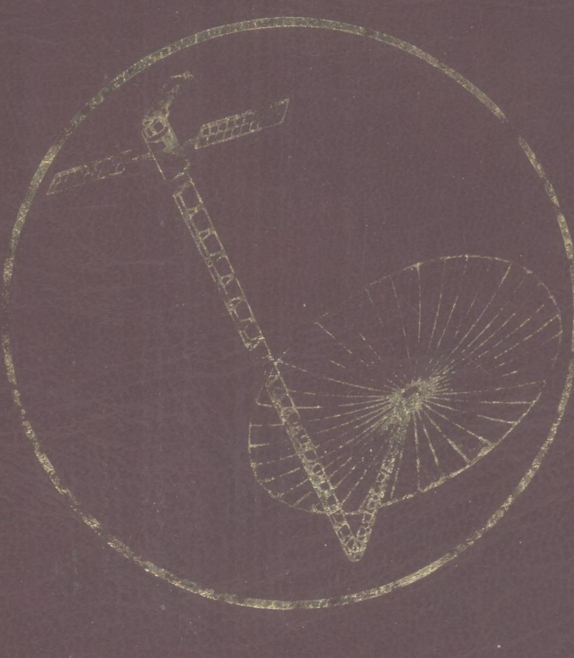

ADVANCES AND TRENDS IN STRUCTURAL AND SOLID MECHANICS

Papers presented at the Symposium on Advances and Trends in Structural and Solid Mechanics

Held 4–7 October 1982, Washington, D.C.

Editors
AHMED K. NOOR
Professor of Engineering and Applied Science, The George Washington University Center at NASA Langley Research Center, Hampton, Virginia, U.S.A.

JERROLD M. HOUSNER
Aerospace Engineer, Structures and Dynamics Division, NASA Langley Research Center, Hampton, Virginia, U.S.A.

Sponsored by the George Washington University and NASA Langley Research Center in cooperation with the National Science Foundation, the Air Force Office of Scientific Research, Office of Naval Research, the American Society of Civil Engineers, and the American Society of Mechanical Engineers.

PERGAMON PRESS

OXFORD · NEW YORK · TORONTO
SYDNEY · PARIS · FRANKFURT

U.K.	Pergamon Press Ltd., Headington Hill Hall, Oxford OX3 0BW, England
U.S.A.	Pergamon Press Inc., Maxwell House, Fairview Park, Elmsford, New York 10523, U.S.A.
CANADA	Pergamon Press Canada Ltd., Suite 104, 150 Consumers Road, Willowdale, Ontario M2J 1P9, Canada
AUSTRALIA	Pergamon Press (Aust.) Pty. Ltd., P.O. Box 544, Potts Point, N.S.W. 2011, Australia
FRANCE	Pergamon Press SARL, 24 rue des Ecoles, 75240 Paris, Cedex 05, France
FEDERAL REPUBLIC OF GERMANY	Pergamon Press GmBH, Hammerweg 6, Postfach 1305, 6242 Kronberg-Taunus, Federal Republic of Germany

ISBN 0 08 029990 3

Published as a special issue of the journal *Computers & Structures*, Vol. 16, Numbers 1–4 and supplied to subscribers as part of their normal subscription. Also available to non-subscribers.

Computers & Structures Vol. 16, No. 1–4, pp. vii–viii, 1983
Printed in Great Britain.
0045–7949/83/010vii–02$03.00/0
Pergamon Press Ltd.

PREFACE†

The field of structural and solid mechanics has witnessed significant and far-reaching advances, on a broad front, in the last decade. The new advances are manifested by the development of new material laws, new structural theories, sophisticated mathematical models, efficient discretization techniques, and numerical algorithms as well as versatile and powerful software systems for structural analysis and design. The driving force behind these activities has been, and continues to be, the need for realistic modeling, accurate analysis and efficient design of large complex structures subject to harsh environments. However, the rapid pace of the development is largely due to the opportunities provided by the extensive advances in computer hardware and software technology as well as the growing interaction among a number of disciplines including applied mechanics, numerical analysis, software design and structural engineering.

As a means of communicating recent advances and as a step towards stronger interaction among applied mechanicians, numerical analysts and structural engineers, a four-day symposium entitled, "Recent Advances and Trends in Structural and Solid Mechanics," was held in Washington, D.C. on 4–7 October 1982. The organizing committee expected that by bringing together leading experts and active researchers in areas which could impact future developments in structural and solid mechanics, formal presentations and personal interaction would increase communication among the disciplines and foster effective development of the technology.

The format of the present symposium differs in a number of ways from the preceding two symposia organized by the George Washington University and NASA Langley Research Center in 1978 and 1980. First, the length of the symposium is extended to four days and more time is provided for informal discussions. Second, three general sessions are organized in three key areas of the structural and solid mechanics discipline, namely: mechanics of materials, finite element technology, and classical analytical techniques and their computer implementation. The third area is also the subject of another session and is given special attention in the present symposium. The editors feel that classical analytical techniques can be combined with contemporary numerical and finite element methods to form effective solution procedures for many structural and solid mechanics problems.

Most of the papers presented at the symposium which report completed research work are contained in this proceedings volume. A companion NASA Conference Publication entitled, "Research in Structural and Solid Mechanics," (1982), contains twenty-six papers presented at the symposium. These papers are primarily short papers reporting research in progress.

The fifty-nine papers contained in this volume document clearly the strides made in various aspects of the structural and solid mechanics discipline and help identify future directions of developments in this field. The topic headings in the symposium are largely represented by the section headings of this volume, namely: (1) Mechanics of Materials and Material Characterization; (2) Advances and Trends in Finite Element Technology; (3) Classical Analytical Techniques and Their Computer Implementation; (4) Interactive Computing and Computational Strategies for Nonlinear Problems; (5) Advances and Trends in Numerical Analysis; (6) Design-Oriented Analysis, Artificial Intelligence and Optimization; (7) Database Management Systems and CAD/CAM; (8) Space Structures and Vehicle Crashworthiness; (9) Beams, Plates and Fibrous Composite Structures; (10) Contact Problems, Random Waves and Lifetime Prediction; and (11) Earthquake Resistant Structures and Other Advanced Structural Applications. The papers contained in this volume will also appear in a special issue of the Journal of Computers and Structures.

The fields covered by the symposium are rapidly changing, and if new results and anticipated future directions are to have maximum impact and use, it is imperative that they reach workers in the field as soon as possible. This consideration led to the decision to publish these proceedings prior to the symposium. Special thanks go to Pergamon Press for their cooperation in publishing this volume and to

†The Publisher apologises to Authors that some articles have been published without authors' corrections being received in order to produce the Proceedings in time for the Conference.

Dean Harold Liebowitz, School of Engineering and Applied Science of the George Washington University for making arrangements for the publication.

The editors are indebted to the many individuals who contributed to the planning of the symposium, in particular to the members of the technical program committee and to the symposium secretary, Mrs. Mary Torian. Special thanks go to the authors of the papers and the referees of the abstracts. The assistance of the National Science Foundation, the Air Force Office of Scientific Research, the Office of Naval Research, the American Society of Mechanical Engineers and the American Society of Civil Engineers are especially appreciated.

The George Washington University Center
at NASA Langley Research Center
Hampton, Virginia, U.S.A.

AHMED K. NOOR
JERROLD M. HOUSNER

CONTENTS

ADVANCES AND TRENDS IN STRUCTURAL AND SOLID MECHANICS

1
Mechanics of Materials and Material Characterization

Computers & Structures Vol. 16, No. 1–4, pp. 3–12, 1983
Printed in Great Britain.

0045-7949/83/010003-10$03.00/0
Pergamon Press Ltd.

MICROMECHANICS

BERNARD BUDIANSKY
Division of Applied Sciences, Harvard University, Cambridge, MA 02138, U.S.A.

Abstract—A brief survey is given of recent and current theoretical studies in the area of micromechanics. Topics discussed include void collapse, transformation toughening, fiber kinking and thermoelastic dissipation. The examples discussed illustrate the use of continuum-mechanical concepts to deduce information concerning constitutive and strength characteristics of metals, ceramics, composites, and rocks.

INTRODUCTION

The area of micromechanics—the mechanics of very small things—has been receiving increasing attention from the mechanics community in recent years. Without attempting to explore the sociology of this trend, this paper will present a brief survey of a variety of problems of micromechanics that are currently of interest.

Micromechanical analyses often have as their goal the deduction via continuum mechanics of rules of macroscopic constitutive behavior. There is poetic justice in this, since constitutive relations, in turn, are indispensible ingredients of continuum mechanics. But other kinds of micromechanical investigations have as their focus the involvement of microscopic inhomogeneities in various kinds of material failure processes. In the studies to be surveyed here, several kinds of microscopic features will be contemplated (voids, inclusions, fibers, crystals); each of the studies will be primarily relevent to a different kind of material (metals, ceramics, composites, rocks); and a variety of phenomena will be considered (void collapse, phase-transformation toughening, fiber-kinking, thermoelastic dissipation). Analyses will be outlined, with details omitted, and implications of results discussed briefly.

VOID COLLAPSE

It has been accepted for some time that ductile failure of metals, both at room temperature under increasing load and at elevated temperature via creep, often involves the growth and coalescence of microscopic voids. On the other hand, the collapse of voids is an essential feature of the compaction of collections of fine metallic particles in powder-metallurgy processing. Some basic studies of void growth and collapse in viscous solids were recently given in Refs. [1–3]; the collapse calculations will be outlined here.

Consider a non-linear, incompressible viscous material obeying, in simple tension, the constitutive relation between stress σ and strain-rate $\dot{\epsilon}$

$$\frac{\dot{\epsilon}}{\dot{\epsilon}_0} = \left(\frac{\sigma}{\sigma_0}\right)^n. \qquad (1)$$

Here $\dot{\epsilon}_0$ and σ_0 are reference strain-rate and stress parameters. The assumed polyaxial generalization of (1) is

$$\frac{\dot{\epsilon}_{ij}}{\dot{\epsilon}_0} = \frac{3}{2}\left(\frac{\sigma_e}{\sigma_0}\right)^{n-1}\left(\frac{s_{ij}}{\sigma_0}\right) \qquad (2)$$

where $s_{ij} = \sigma_{ij} - \frac{1}{3}\sigma_{kk}\delta_{ij}$ is the stress deviator, and $\sigma_e = (3s_{ij}s_{ij}/2)^{1/2}$ is the effective stress. The following fundamental void-collapse problem was considered in [3]: under the remote, axisymmetric, constant stresses $\sigma_{11} = S$, $\sigma_{22} = \sigma_{33} = T$ $(S \le 0,\ T \le 0)$, what is the history of deformation undergone by a single, isolated, initially spherical void?

The case of *linear* creep $(n = 1)$ was easily solved in [1] on the basis of the famous Eshelby solution[4] for an isolated, elastic ellipsoidal inclusion in an infinite elastic body. Adapting this solution to the case of linear creep, and making the inclusion vacuous, reveals that the hole undergoes a continuous metamorphosis, via spheroidal shapes, towards either a flat crack (for $|T| < |S|$) or a thin needle (for $|S| < |T|$). Simple differential equations for the evolution of the void-volume V as a function of time emerge from the Eshelby solution, and for fixed values of S/T, these are easily integrated numerically. Time can then be eliminated to provide relationships between the void volume and the overall strain of the material. Some typical results for the two distinct modes of void reduction—pressing $(S/T > 1)$ and squeezing $(S/T < 1)$—are shown in Figs. 1 and 2, wherein void volume is plotted, non-dimensionally, against the overall axial length ratio. Note that zero void-volume is attained at a finite value of shortening when the void is flattened into a crack. However, V vanishes only asymptotically in the squeezing mode.

But now, what about $n > 1$? First of all, there is a real surprise, discovered in [1], about the ranges of S/T corresponding to pressing and squeezing. By means of a Rayleigh–Ritz solution for the *initial* mode of deformation of a spherical void, it was found that for $n > 1.5$,

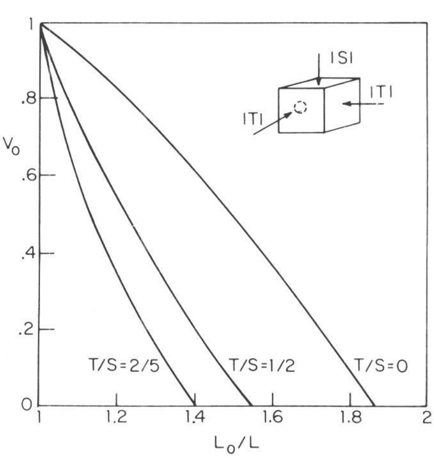

Fig. 1. Void collapse: sphere to crack $(n = 1)$. V_0 and V are the original and current void volumes. L_0 and L are the original and current specimen lengths in the direction of S.

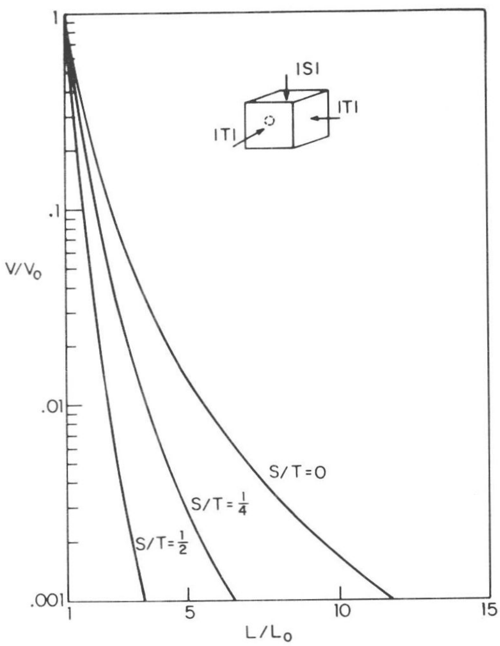

Fig. 2. Void collapse: sphere to needle ($n = 1$).

the void would start to flatten, and head towards crack-like collapse, for a range of values of $S/T < 1$ (see Fig. 3). On the other hand, for some values of $S/T > 1$, the void actually gets skinnier, and starts to turn into a needle. But regardless of the final configuration towards which the void tends, calculating its history is not easy, and so some estimation procedures were devised in [3]. In effect, approximate differential equations for the void volume were written on the basis of interpolations between the volumetric rates-of-change for spherical holes found in [1], and those for either asymptotic needles or cracks.

For needle-like cavities, the dilatation rate $\dot{V}/V$ is related to S/T by the neat formula

$$S/T = 1 + \left\{\frac{1}{\sqrt{3}}\int_0^{\dot{V}/(\sqrt{(3)}\,\dot{\epsilon}V)} [1 + x^2]^{(1-n)/2n}\right\}^{-1} \tag{3}$$

also discovered in [1]. Here $\dot{\epsilon} = \dot{\epsilon}_0|(S-T)/\sigma_0|^{n-1}((S-T)/\sigma_0)$ is the remote axial strain-rate. The analogous information for crack-like cavities was estimated on the basis of the numerical results of He and Hutchinson on fully plastic, mode I penny-shaped cracks[5]. The approximate interpolative procedures desired were checked out for the case $n = 1$ and found to be reasonably accurate. Some typical results for $n > 1$ are shown in Fig. 4 for pure pressing ($T = 0$); in Fig. 5 for pure squeezing ($S = 0$); and in Fig. 6, with $n = 5$, for several values of S/T. In this last case, the limiting configurations go from crack to needle to crack to needle as T/S varies from zero to infinity. Despite this, the individual curves follow in orderly progression.

It is evident that results such as these provide only the beginnings of a quantitative understanding of real void-compaction processes, ignoring as they do many possibly important effects of void interaction, non-ideal void geometry, mass-diffusion effects, and so on. The analogous problems for time-independent, strain-hardening plasticity are largely unexplored, although it may be hoped that some of the purely geometrical relations discussed for voids in viscous metals may carry over, approximately, to time-independent plasticity.

TRANSFORMATION TOUGHENING

Transformation toughening is a phenomenon that has excited the attention of many ceramists in the last few years[6, 7]. Ceramics have admirable high-temperature properties (in fact, this almost defines a ceramic) but they tend to have low fracture toughness. Transformation toughening depends on the reinforcement of one ceramic with tiny particles of another (e.g. zirconia, ZrO_2) that are susceptible to a dilatant phase transformation when they are subjected to a critical triggering stress. The idea is this: in the vicinity of a crack tip, elevated stresses will cause the particles to transform, expand in volume—and hence tend to close the crack! But, as we shall see, the situation is not quite that simple[8, 9].

Suppose that the particles obey the tri-linear relation shown in Fig. 7(a) between mean stress $\sigma = \frac{1}{3}\sigma_{ii}$ and dilatation $\theta = \epsilon_{ii}$. Under increasing σ, the phase transformation would occur suddenly at the critical mean stress σ^c, and a jump $\theta_P{}^T$ in dilatation would occur. (In general, the phase transformation would also involve shearing deformation, ignored here.) However, under suitably prescribed histories of mean stress and dilatation, the three branches of the $\sigma - \theta$ relation may be traversed continuously. The slope of branches 1 and 3 is B, the bulk modulus; the slope of the intermediate branch is B'. The particles are assumed isotropic, with shear modulus G.

If a collection of these particles is distributed ran-

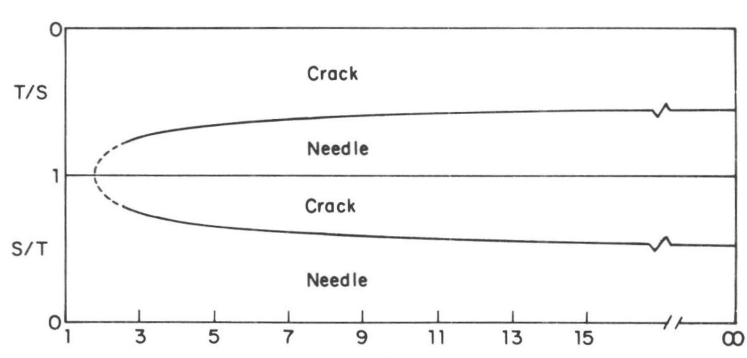

Fig. 3. Predicted collapse configurations of initially spherical voids.

domly, with volume concentration c, in a non-transforming matrix having the same bulk and shear moduli, the effective macroscopic $\sigma-\theta$ relation of the composite will be as shown in Fig. 7(b). The slopes of the initial and final branches remain equal to B, but the intermediate branch has a slope $\bar{B}$ related to B' by

$$(\bar{B}+4G/3)^{-1}=c(B'+4G/3)^{-1}+(1-c)(B+4G/3)^{-1}. \tag{4}$$

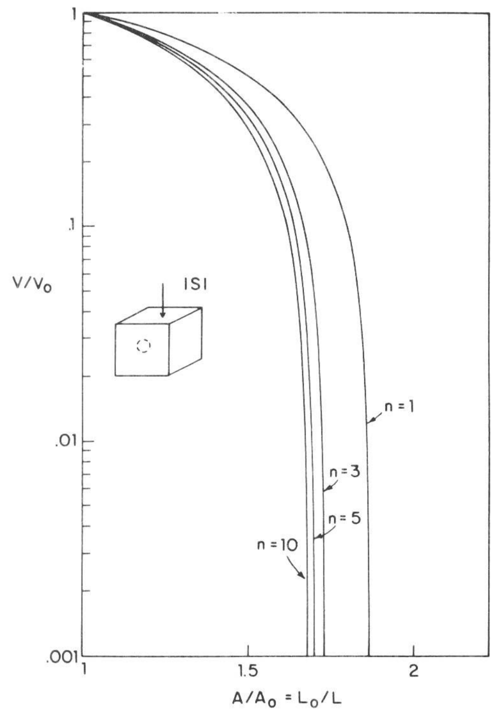

Fig. 4. Void collapse: sphere to crack ($S<0$, $T=0$). A_0 and A are the original and current cross-sectional areas of the specimen normal to the direction of S.

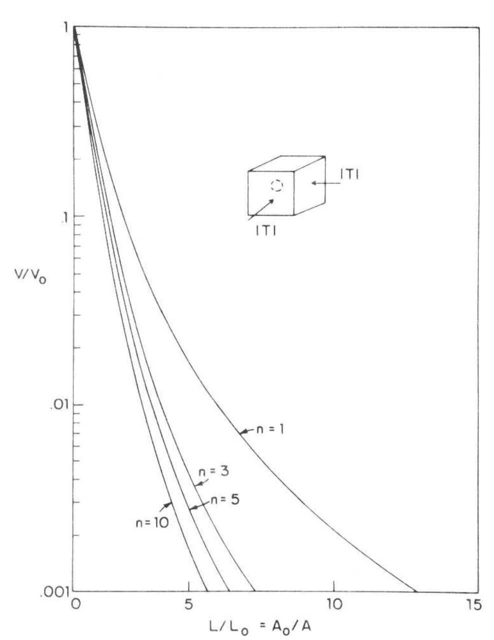

Fig. 5. Void collapse: sphere to needle ($S=0$, $T<0$).

This is an *exact* result, independent of particle shape. Also, the shear modulus of the composite is exactly G, and the critical stress of the composite stays equal to σ^c. The maximum overall dilatation θ^T due to the phase transformation is given by

$$\theta^T=c\theta_P{}^T \tag{5}$$

and this is also exact. The form of eqn (4) suggests that something special might happen for $\bar{B}=B'=-4G/3$; this will be verified shortly.

We can now study plane-strain crack-tip stress intensity factors consistent with the $\sigma-\theta$ constitutive relation of Fig. 7(b) to see whether, and how much, they have been reduced by the kind of phase transformation this relation embodies. By analogy with the well-known *small-scale yielding* problem of fracture mechanics, one can introduce the idea of *small-scale transformation* (see Fig. 8a), wherein the transformed zone around a crack tip is very small relative to crack length and all other geometric variables. Far enough away from the crack tip, the stresses are proportional to the nominal, elastic stress-intensity factor K, with the usual $1/\sqrt{r}$ variation. Near the tip, at a *stationary* crack, one can

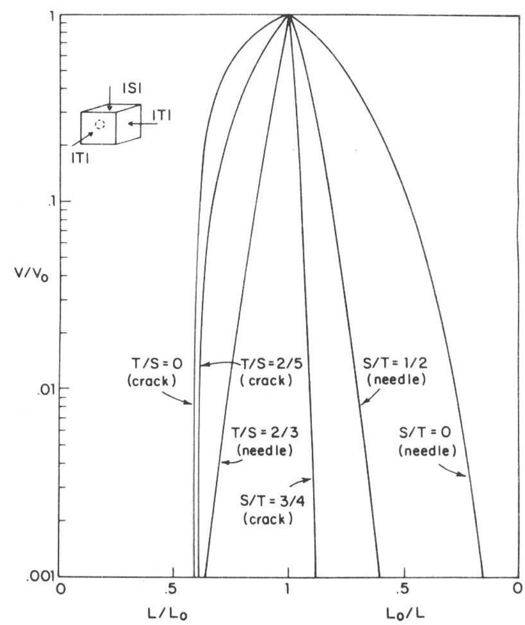

Fig. 6. Collapse of spherical voids, $n=5$.

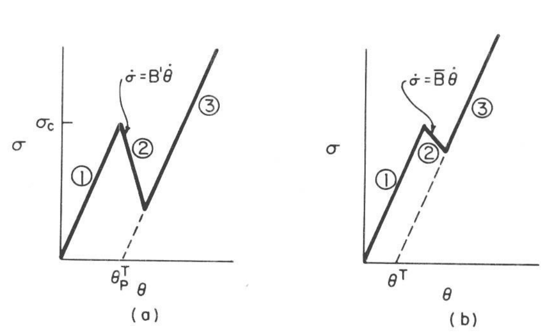

Fig. 7. Volumetric constitutive relations, (a) particles, (b) composite.

expect the particles to be transformed within regions like those shown shaded in Fig. 8(a). The circled numbers denote corresponding segments in the $\sigma-\theta$ curve of Fig. 7(b). Thus, in region 3 the particles are fully transformed, in region 2 only partially, and in region 1 not at all.

Now let K_{tip} denote the *actual* stress-intensity factor at the crack-tip, which is embedded in region 3. The startling conclusion can be drawn [8, 9] that $K_{tip} = K$! In other words, there is *no* net alleviating effect of all the particle expansions on the stress intensity, and hence no transformation toughening of a stationary crack. As it turns out, the toughening resides in the crack *stopping* capacity of the transformed particles, rather than in the prevention of crack initiation. Thus (Fig. 8b) the study of a steadily growing crack in [9] indicates wake regions of transformed particles that *do* tend to close the crack tip, and produce $K_{tip} < K$. (This rests on the assumption that once the particles transform, they do not untransform back to their original states.)

Various methods have been used in [9] to calculate K_{tip} for the growing crack. The easiest applies to the case in which there is no region 2 at all, the particles being either fully transformed or not at all. In turn, the condition for this to happen is $\bar{B} \le -4G/3$ (or, for a backward-slanting branch 2, $\bar{B} > B$). For this *supercritical* case, a rigorous analytical asymptotic result for K_{tip}/K found in [9] is

$$K_{tip}/K \sim 1 - \frac{3\sqrt{3}}{8}\alpha \tag{6}$$

for sufficiently small values of

$$\alpha = \frac{2(1+\nu)}{9\pi(1-\nu)}\left[\frac{E}{\sigma^c}\right][c\theta_P{}^T]. \tag{7}$$

(The same answer was found numerically in [8].) Also, the wake height H is given asymptotically by

$$H = \frac{\sqrt{(3)}\,(1+\nu)^2}{12\pi}\left[\frac{K}{\sigma^c}\right]^2 \tag{8}$$

so that, in terms of H, the toughening may be estimated by the formula

$$\Delta K \equiv K - K_{tip} = \frac{Ec\theta_P{}^T}{(1-\nu)}\frac{1}{2}\left[\frac{H}{\pi\sqrt{3}}\right]^{1/2} \tag{9}$$

for the reduction in the tip stress-intensity factor.

For $\bar{B}/G > -4/3$, and α not small, finite-element methods were used to calculate K_{tip}/K, with explicit consideration of the zone of partial transformation. The results are shown in Figs. 9 and 10. The analytical estimate (9) for ΔK is very good for $\bar{B} \le -4G/3$, which gives the largest possible toughening effect.

Comparisons in Ref. [9] with several bits of available experimental data suggest that eqn (9) may give only about 1/3–2/3 of the observed toughening effects. Thus, there is plenty of room for better understanding of this interesting, and possibly very useful, phenomenon. In particular, shear strains in the phase transformation may have to be considered, and knowledge of the constitutive rules governing the individual transforming particles would be useful.

FIBER KINKING

Internal buckling of unidirectionally reinforced fibrous composite materials under static or dynamic axial compression has long been recognized as a possible mode of failure. The occurrence of highly localized kinking of microscopic fiber bundles has recently rekindled interest in this type of material instability [10]. Figure 11 shows photographs, under various magnifications, of kink bands (A. G. Evans, 1977) in carbon–carbon composites.

The theoretical literature on kinking is not profuse. Kinking was analyzed as *elastic* shear buckling by Rosen [11] in 1965, who, in effect, found that kinking rotation ϕ (see Fig. 12) in initially straight fibers ($\bar{\phi} = 0$) can start at the critical compressive stress

$$\sigma_c = G \tag{10}$$

where G is an elastic shear modulus of the composite, defined with respect to shearing strain rate relative to the rotating fiber axes. This formula is exact for a kink-band angle of $\beta = 0$, and under the reasonable assumption of inextensional fibers, it has been generalized [12] to

$$\sigma_c = G + E_T \tan^2\beta \tag{11}$$

for $\beta \neq 0$, where E_T is defined in Fig. 12. But eqn (11) gives $\beta = 0$ as the critical angle for kinking—this despite the fact that observed kink angles, while scattered, are usually bounded well away from zero.

Unfortunately, elastic kinking analyses are not relevant to most composites of current interest. The Rosen result is very unconservative when applied to, say, graphite-epoxy or carbon–carbon composites. Furthermore, attempts to salvage elastic kinking on the basis of

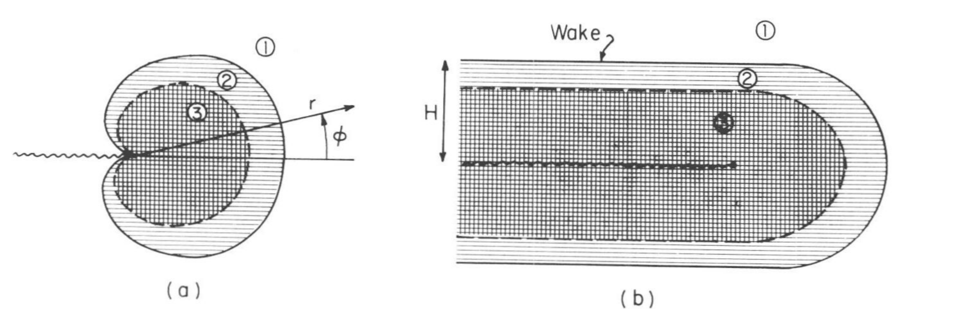

Fig. 8. Transformed-particle regions (2, 3) in (a) stationary crack, (b) steadily growing crack, embedded in the nominal elastic stress field $\sigma_{ij} \sim Kf_{ij}(\phi)/\sqrt{r}$ far from the crack tip.

imperfections fail: zero-angle kinking is imperfection *insensitive*[13] and while there is imperfection-sensitivity for $\beta \neq 0$, it is far too small to provide significant knockdown factors[12].

The situation changes dramatically when we consider plasticity. If we assume perfect plasticity in pure shear beyond $\gamma = \gamma_y = \tau_y/G$, then the maximum stress that can be supported by a zero-angle kink ($\beta = 0$) is

$$\sigma_s = \left[\frac{\gamma_y}{\bar{\phi} + \gamma_y}\right]\sigma_c \tag{12}$$

where $\bar{\phi}$ is an initial imperfection, in the form of a fiber misalignment angle within the assumed kink region. Thus, for example, $\gamma_y = 0.002$ and $\bar{\phi} = 2°$ hits the elastic estimate (10) with a plastic knockdown factor of 1/18. For $\gamma_y \ll \bar{\phi}$, (12) gives the approximation

$$\sigma_s \sim \tau_y/\bar{\phi} \tag{13}$$

which was suggested by Argon[14] in 1972.

Strain hardening in shear hardly changes these results. But what about $\beta \neq 0$? Inclined kink-bands induce trans-

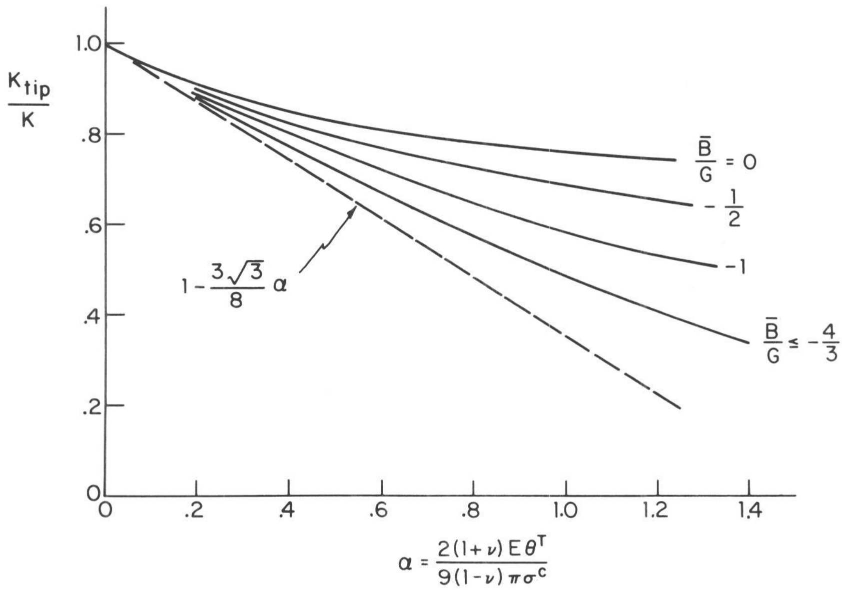

Fig. 9. Ratio of actual to nominal stress-intensity factor. (The curves for $\bar{B}/G > -4/3$ were calculated with $\nu = 0.3$.)

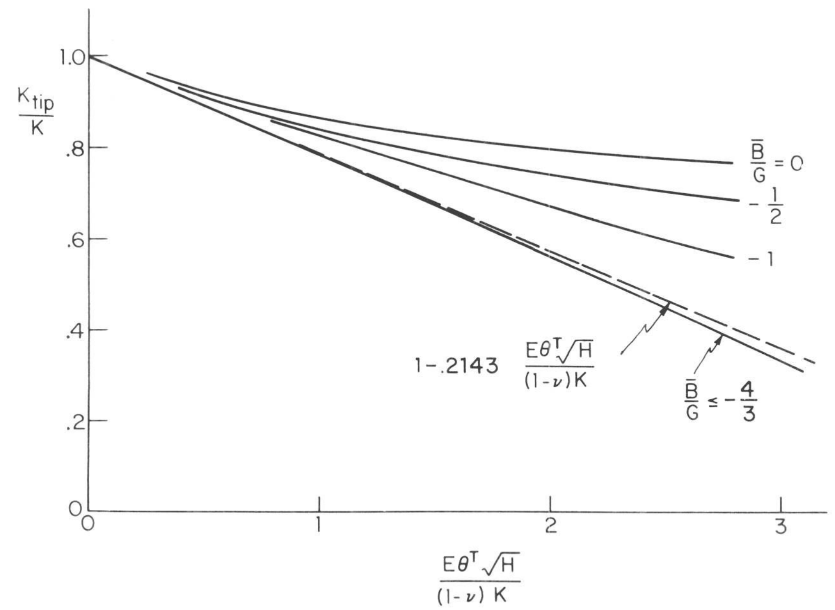

Fig. 10. Ratio of actual to nominal stress-intensity factor. The dashed line is the asymptotic result for small θ^T when $\bar{B}/G \leq -4/3$.

verse stresses at the initiation of kinking, so that a combined-stress plasticity law must be invoked. The arbitrary assumption of a quadratic yield condition (as good as anything in the face of experimental ignorance)

$$\left(\frac{\tau}{\tau_y}\right)^2 + \left(\frac{\sigma_T}{\sigma_{Ty}}\right)^2 = 1 \qquad (14)$$

has been used to study inclined kinking, together with the mathematical assumption-of-convenience $E_T/G = (\sigma_{Ty}/\tau_y)^2$. The result for the maximum compressive stress is

$$\sigma_s = \left[\frac{\gamma_y}{\bar{\phi}\sqrt{\left(\frac{\sigma_c}{G}\right) + \gamma_y}}\right]\sigma_c. \qquad (15)$$

So, for a given $\bar{\phi}$, misalignments within an inclined band produce a larger reduction of the elastic kinking stress than they do for $\beta = 0$. But the knockdown factor now

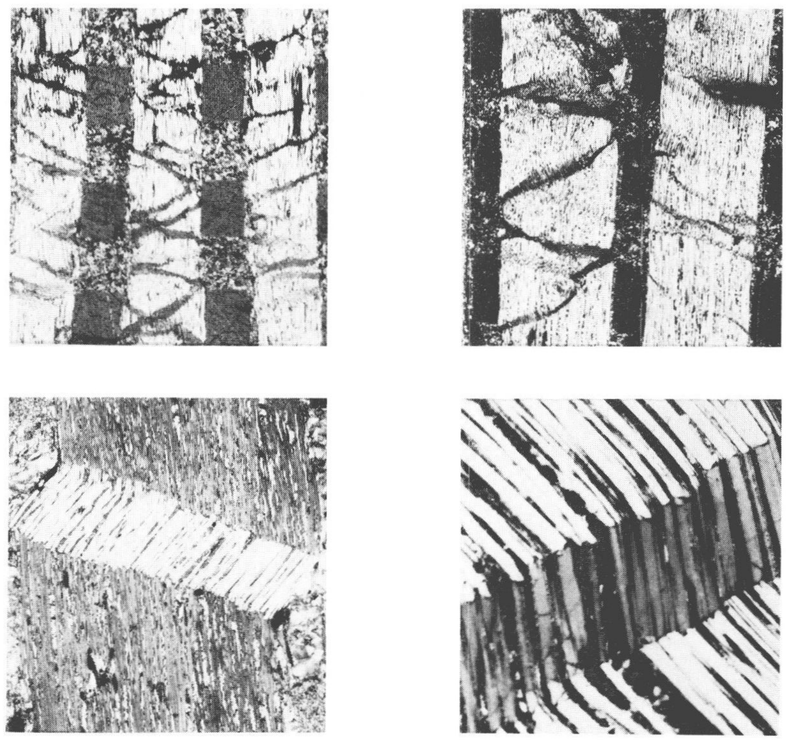

Fig. 11. Kink bands within fiber bundles in carbon–carbon composites. The individual fiber diameters are about 6 μ.

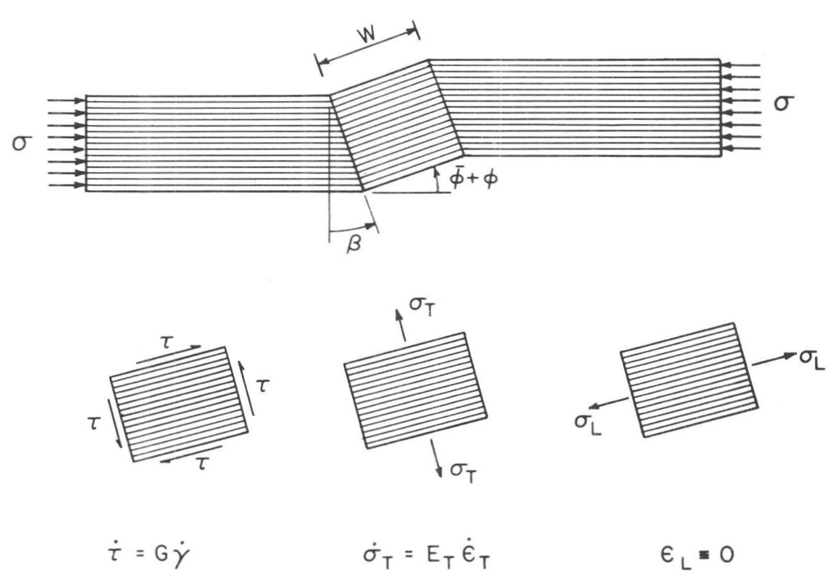

Fig. 12. Kink band notation: dots over stresses represent total time derivatives (*not* Jaumann derivatives); $\dot{\gamma}$, $\dot{\epsilon}_T$, $\dot{\epsilon}_L$ are velocity-strains.

acts on the bigger σ_c given by (11), and the net effect is that for comparable values of misalignment, zero-angle kinking is still predicted.

At this point, we can reasonably conclude that the most important parameters affecting the kink strength of real composites have probably been identified. High stiffness and strength in shear are clearly desirable, and the sensitivity to fiber misalignment is very great. (Hence large scatter in kinking strengths may be expected.) But a nagging question remains: why are large kink angles, up to 40° or so, persistently observed, and small kink angles rarely? Can we be sure that we *really* understood the kinking mechanism if we ignore this question? The answer that suggests itself is that, for some reason, the patterns of initial misalignment that induce plastic kinking tend to arrange themselves into inclined bands; but why? A simple analysis of the elastic effects of localized boundary imperfections provides an answer.

Elastic, plane-strain, inextensional deformation of the compressed composite gives displacements $v(x, y)$ normal to the fibers governed by the p.d.e.

$$\left(1-\frac{\sigma}{G}\right)\frac{\partial^2 v}{\partial x^2}+\frac{E_T}{G}\frac{\partial^2 v}{\partial y^2}=\left(\frac{\sigma}{G}\right)\frac{\partial^2 v_0}{\partial x^2} \qquad (16)$$

where $v_0(x, y)$ is an initial displacement pattern. If we contemplate the half-plane $y \geq 0$, the effect of a highly localized, very short-wave imperfection at the boundary may be simulated by

$$v_0=\delta(x)\delta(y) \qquad (17)$$

where the δ's are Dirac delta functions. On the other hand, a very long-wave imperfection, still concentrated at the edge $y=0$, may be represented by

$$v_0=-|x|\,\delta(y). \qquad (18)$$

The long-wave imperfection leads to a solution for $\phi \equiv \partial v/\partial x$ proportional to

$$-\frac{x}{x^2+y^2\left(\dfrac{G-\sigma}{E_T}\right)} \qquad (19)$$

and this corresponds to a locus of $|\phi|_{\max}$ along the lines

$$x=\pm y\sqrt{\left(\frac{G-\sigma}{E_T}\right)}. \qquad (20)$$

Similarly, the short-wave imperfection gives $|\phi|_{\max}$ along

$$x=\pm y(\surd(2)-1)\sqrt{\left(\frac{G-\sigma}{E_T}\right)}. \qquad (21)$$

The implications are evident: localized deviations from ideal fiber alignment (e.g. due to inclusions, voids, fiber spacing irregularities) having no particular geometrical bias *induce* patterns of angular misalignment due to elastic distortion that arrange themselves into inclined domains. These rotations then induce plastic kinking into similarly inclined kink bands.

Failure follows rapidly after plastic deformation begins, so that it is reasonable to identify σ in eqns (20) and (21) with the kinking failure stress σ_s. The consequent correlations between σ_s and the kink angle β that follow are

$$\tan\beta=\pm\sqrt{\left(\frac{1-\sigma_s/G}{E_T/G}\right)} \quad \text{(long-wave imperfections)} \qquad (22a)$$

$$=\pm(\surd(2)-1)\sqrt{\left(\frac{1-\sigma_s/G}{E_T/G}\right)} \quad \text{(short-wave imperfections).} \qquad (22b)$$

Hence, for the values $E_T/G=2$ and 4, the kink angles to be expected should fall in the shaded regions shown in Fig. 13. So, kink angles less than 10° and greater than 35° should be infrequent. It may be noted, too, that the frequent occurrence of twinned kink bands in the upper photographs of Fig. 11 is consistent with the $\pm\beta$ loci of $|\phi|_{\max}$ emanating from local imperfections.

There is still something else that begs to be addressed: the kink width W (Fig. 12). To find a rational estimate, we must change our micromechanical focus, and take individual fiber dimensions into account. Indeed, it seems evident that the fiber diameter d is the only meaningful characteristic size in the problem. The final observed kink width is clearly delineated by bending breaks in the fibers, so that local fiber bending resistance, hitherto ignored, must be considered explicitly. The fibers may, accordingly, be considered to undergo *inextensional bending* until they break. At the same time, the elastic strain of the matrix can be neglected with respect to its plastic strain, i.e. the matrix is assumed rigid-plastic. Smearing out the fibers then leads to a simple couple-stress formulation which gives no fiber rotations at all outside an inclined band, and the possibility of rotations

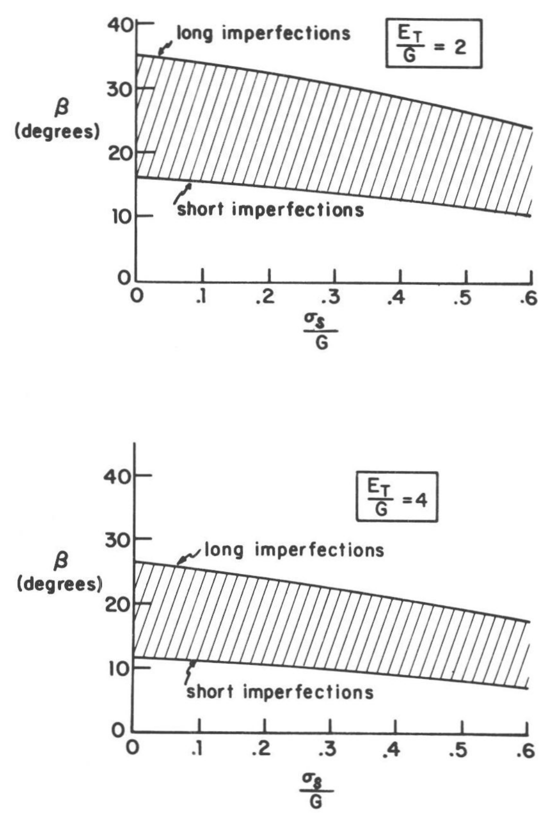

Fig. 13. Estimated kink-band inclinations.